MOLECULAR AND CELLULAR BIOLOGY, Nov. 2002, p. 7484–7490 Vol. 22, No. 21
0270-7306/02/$04.00+0 DOI: 10.1128/MCB.22.21.7484–7490.2002

hSWI/SNF-Catalyzed Nucleosome Sliding Does Not Occur Solely via a Twist-Diffusion Mechanism

Sayura Aoyagi and Jeffrey J. Hayes*

Department of Biochemistry and Biophysics, University of Rochester Medical Center, Rochester, New York 14642

Received 21 June 2002/Accepted 6 August 2002

Nucleosome remodeling by the hSWI/SNF complex and other chromatin remodeling complexes can cause translocation (sliding) of the histone octamer in *cis* along DNA. Structural and biochemical evidence suggest that sliding involves a DNA twist-diffusion process whereby the DNA rotates about the helical axis without major displacement from the surface of the nucleosome and that this process may be driven by torsional stress within the DNA. We report that hSWI/SNF efficiently catalyzes sliding of nucleosomes containing branched DNAs as steric blocks to twist-diffusion and a nick to allow dissipation of torsional stress within the nucleosome. These results suggest that SWI/SNF-catalyzed nucleosome sliding does not occur exclusively via a simple twist-diffusion mechanism and support models in which the DNA maintains its rotational orientation to and is at least partially separated from the histone surface during nucleosome translocation.

The orderly and efficient packaging of DNA within the eukaryotic cell nucleus into nucleosomes and higher-order chromatin structures greatly restricts the availability of DNA for nuclear processes (38). To utilize genomic DNA within this restrictive environment, cells have developed several mechanisms to facilitate access of *trans*-acting factors to DNA targets within chromatin (39, 41). Posttranslational modifications of the histone proteins such as acetylation and methylation may serve to directly alter the biochemical characteristics of chromatin or to signal the binding of ancillary factors (17, 32, 42). In addition, critical DNA elements are exposed by active disruption of histone-DNA interactions by ATP-dependent chromatin remodeling complexes (18, 35, 41).

The multisubunit SWI/SNF complex is the archetypal member of a family of closely related chromatin remodeling complexes and is known to play a key role in regulation of chromatin accessibility in vivo (8, 9; reviewed in reference 28). However, the mechanism by which SWI/SNF chromatin remodeling complexes utilize the energy of ATP hydrolysis to perturb histone-DNA interactions is not well defined (6, 7, 14, 19, 24). Remodeling occurs without large changes in either the conformation or the configuration of the core histone octamer (2, 4). However, electron energy loss microscopy and atomic force microscopy of remodeled nucleosome arrays indicate that approximately 40 bp of DNA-histone contacts are destabilized at either edge in a remodeled nucleosome (2, 31). Moreover, recent evidence indicates that many remodeling complexes can impart torsional stress into DNA, thereby inducing disruption of histone-DNA interactions (10, 13). However, nucleosome sliding induced by the ISWI chromatin remodeling enzyme occurs readily on nicked DNA; thus, the role of torsional stress in at least some remodeling processes remains unclear (20).

A number of ATP-dependent chromatin remodeling activities have been shown to catalyze nucleosome translocation (sliding) along the DNA in *cis* for both mononucleosomes and nucleosome arrays (11, 12, 16, 21, 36). Remodeling-dependent octamer translocation along the DNA leads to exposure of DNA sites previously occluded by histones, thereby facilitating the binding of *trans*-acting factors to DNA (18, 41). Indeed, SWI/SNF-catalyzed nucleosome sliding is thought to be a significant manifestation of remodeling activities in vivo (16, 36, 37). However, SWI/SNF-mediated remodeling has also been observed on short, single-nucleosome-sized DNA templates which are likely to restrict octamer mobility (10, 15, 16). In addition, a nucleosome in which H2A is covalently cross-linked to nucleosomal DNA is still efficiently remodeled by hSWI/SNF as determined by disruption of the DNase I digestion pattern (23). Thus, at least some aspects of nucleosome remodeling (i.e., hSWI/SNF-catalyzed disruption of histone-DNA interactions) can occur in the absence of hSWI/SNF-catalyzed nucleosome sliding. Indeed, recent results suggest that hSWI/SNF causes both sliding and disruption of nucleosome structure on nucleosome arrays (31) and that hSWI/SNF remodeling of a mononucleosome results in exposure of cognate sites for restriction enzymes at rates that are not easily explained by a sliding mechanism (27). Thus, nucleosome sliding is but one outcome of the as yet undefined mechanism of remodeling. Nonetheless, it is likely that nucleosome sliding serves to increase the stable exposure of critical DNA elements by nucleosome remodeling activities in vivo (18).

Although many processes can be envisaged that will result in nucleosome sliding, two general, non-mutually exclusive models have been proposed that may describe the sliding mechanism (37). In the first, sliding may occur by twisting of the DNA helix like a corkscrew along the surface of the histone octamer. This model is supported by the recent crystal structure of a nucleosome core in which a turn of DNA near the periphery of the core contains one additional base pair compared to the symmetry-related position on the opposite side of the core (25). It has been hypothesized that such extra base pairs may stochastically diffuse throughout the structure, thus advancing the histone octamer along the DNA one base pair at a time

* Corresponding author. Mailing address: Department of Biochemistry and Biophysics, University of Rochester Medical Center, Rochester, NY 14642. Phone: (716) 273-4887. Fax: (716) 271-2683. E-mail: jjhs@uhura.cc.rochester.edu.

(37). The cumulative effect of several base pairs diffusing in the same direction would be a screwing of the DNA along the histone surface, such that the DNA maintains its writhe. This model has the advantage that the majority of histone-DNA interactions are maintained at any one point in time. In addition, a DNA uncoiling-recapture mechanism may also contribute to nucleosome sliding (37). Out-of-register recapture of an uncoiled segment of nucleosomal DNA would generate a DNA loop, which could then be translated through the rest of the nucleosome in a wave-like motion. We have tested if hSWI/SNF-dependent nucleosome sliding involves a DNA twist-diffusion process by examining sliding of nucleosomes containing branched and nicked DNAs that would sterically hinder rotation of the DNA on the octamer surface and inhibit retention of torsional stress within the helix. Remodeling of these nucleosomes suggests that the mechanism of hSWI/SNF-catalyzed nucleosome sliding does not involve significant amounts of DNA twist-diffusion or rotation of DNA on the nucleosome surface.

MATERIALS AND METHODS

DNA fragments. All DNA fragments are based on the 215-bp *Eco*RI-*Dde*I fragment containing a *Xenopus borealis* somatic 5S RNA gene derived from the plasmid pXP-10 (1). A corresponding fragment containing a *Hha*I site at position +123 was generated by PCR (all positions numbered with respect to start site for transcription of the 5S gene) with *Eco*RI-digested pXP-10, primer DRC5S-66 (5′AAT TCG AGC TCG CCC CGG GAT CCG GCT GGG CCC CCC CCA GAA GGC AGC ACA AGG GGA GGA AAA GTC3′), and 5′-radiolabeled primer SA5S-PCR1-*Hha*I (5′TCA GAA TGG CAA AAG CGC GAA AGC C3′). The double-stranded DNA fragment extending from positions −78 to +137 in the 5S sequence and radiolabeled at the downstream 5′ end was purified on a 6% native polyacrylamide gel. Hairpin, flap, and nicked substrates were prepared in two steps. First, a continuous bottom strand for all three, extending from positions −78 to +137 in the 5S sequence, was generated, ligating three oligonucleotides, containing bottom-strand 5S sequences +140 to +69, +68 to −4, and −4 to −74, identical to sequences in the native fragment derived from XP-10. Four hundred fifty picomoles of each oligonucleotide was treated with ATP by using T4 polynucleotide kinase (New England Biolabs); then annealed with 900 pmol each of two bridging oligonucleotides, ACGATATCGGGCAGT TTCAGGGTGGTATGGCCGTAGGCGA and GGCGGTCTCCCATCCAAG TACTAACCAGGCCCGACCCTGC; and ligated with T4 DNA ligase (Gibco BRL) as described previously (5). The product of this ligation reaction (215-mer) was isolated with a preparative denaturing polyacrylamide gel (6%) after visualization of the bands by ethidium bromide staining. The downstream portions of the top strand of the hairpin, flap DNA, and nicked templates were created by ligating 450 pmol each of either GAC CAG GAG GGG TTT TTC CCC TCC TGG TCA GAG CCT TGT GCT CGC CTA CGG CCA TAC CAC C (hairpin), TCC CCT CCT TTT CAG AGC CTT GTG CTC GCC TAC GGC CAT ACC ACC (flap), or AGC CTT GTG CTC GCC TAC GGC CAT ACC ACC (nicked) with GTG AAA GTG CCC GAT ATC GTC TGA TCT CGG AAG CCA AGC AGG GTC GGG CCT GGT TAG and TAC TTG GAT GGG AGA CCG CCT GGG AAT ACC AGG TGT CGT AGG CTT TTG CAC TTT TGC CAT TC. The oligonucleotides were annealed with 900 pmol each of two bridging oligonucleotides, ACG ATA TCG GGC AGT TTC AGG GTG GTA TGG CCG TAG GCG A and GGC GGT CTC CCA TCC AAG TAC TAA CCA GGC CCG ACC CTG C, and then ligated with T4 ligase as described above. The products of the ligation reactions (180-mer for hairpin DNA, 164-mer for flap DNA, and 149-mer for nicked DNA) were isolated with preparative denaturing polyacrylamide gels (6%) after visualization of the bands by ethidium bromide staining. All three ligation products (top downstream strands) are identical to positions −12 to +137 on the top strand of the 215-bp native 5S template. Finally, double-stranded flap, hairpin, and nick templates were generated by annealing the three strands generated above in three separate annealing reactions with the 66-mer DRC5S-66 oligonucleotide and 215-mer bottom-strand DNA prepared as described above. In addition, an excess of a 13-mer, GAA AAG GAG GGG A3′, which anneals to the first 5′ 13 nucleotides of the 164-mer to form a double-stranded flap, was added to the flap template reaction. The mixtures were heated to 95°C for 5 min and cooled slowly by turning off the heating block. The annealing reactions created a 215-bp double-stranded 5S DNA with either a hairpin (12-bp stem and a 5-nucleotide loop) or a 13-bp double-stranded flap with a 2-nucleotide hinge at the −12 position or a nick at position −12 (Fig. 1A). For *Hha*I digestions and hydroxyl radical footprinting the 215-mer bottom strand was 5′ radiolabeled prior to the annealing reaction. For the *Eco*RV reaction, the top downstream primers were 5′ radiolabeled prior to the annealing reaction. For the DNase I assay, the bottom 215-mer strand was 3′ end labeled with the Klenow fragment (New England Biolabs) prior to the annealing reaction.

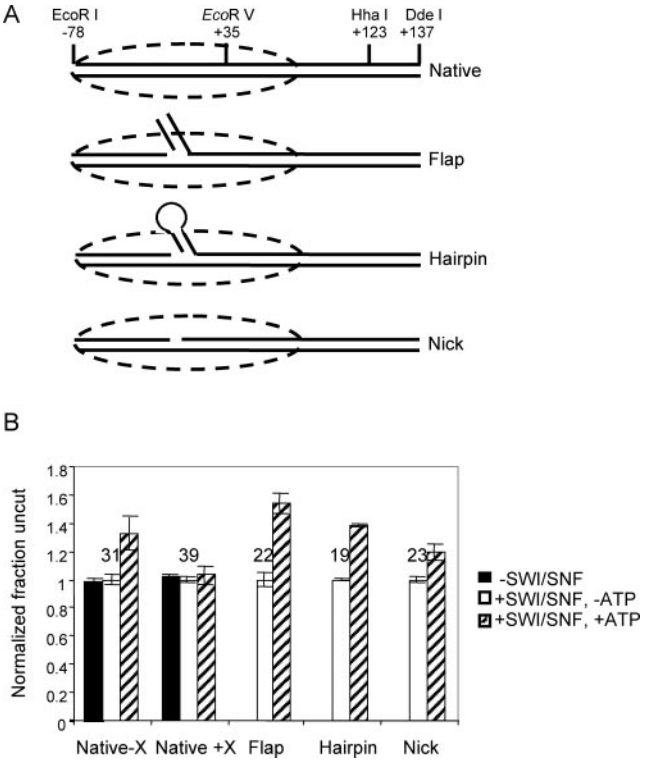

FIG. 1. hSWI/SNF-catalyzed octamer sliding is not inhibited by branched DNA structures within the nucleosome. (A) DNA fragments used for nucleosome reconstitution. The flap, hairpin, and nick substrates contain the same sequences as the 215-bp intact fragment. The positions of the branch site, relevant restriction enzyme sites, and the main region of DNA assembled into the nucleosome (oval) are shown. (B) Nucleosome sliding assay. Purified nucleosomes prepared with native, flap, hairpin, and nicked DNAs were incubated in the absence of SWI/SNF (solid bars) or with hSWI/SNF without ATP (open bars) or with ATP (hatched bars) for 15 min and then subjected to *Hha*I digestion for 10 min. The bar graph shows the fraction of DNA remaining uncut after *Hha*I digestion, normalized to the amount remaining in the controls without SWI/SNF. Data were normalized in this manner since the fraction of nucleosomes remaining undigested (inset numbers) varied slightly between nucleosome preparations. Note that the nucleosomes reconstituted with the native DNA fragment contained H2BG26C-APB and were irradiated to produce portions of the sample that either were not cross-linked (Native-X) or were cross-linked (Native+X). Experiments with native DNA template and native histones produced results identical to those for the Native-X samples (data not shown).

Nucleosome reconstitution. Recombinant *Xenopus* H2A and the cysteine-substituted mutant H2BG26C were prepared as a preformed dimer and reacted with 4-azidophenacylbromide (Sigma) as described previously (1, 22). Core histones H3/H4 were prepared from chicken erythrocyte nuclei, and nucleosomes were reconstituted with either H2A/H2BG26C-APB prepared as described above or H2A/H2B prepared from chicken erythrocyte nuclei. Reconstitution with the 5S DNA fragment from *X. borealis* yields a majority of nucleosomes in which the dyad axis of symmetry is located at position −3 with respect to the

transcription start site of the 5S gene (+1) (40). Reconstitutions were loaded onto 10-ml 5 to 30% glycerol (in 10 mM Tris-Cl, pH 8.0) gradients, and nucleosomes were sedimented at 198,000 × *g* for 18 h at 4°C. Fractions containing the purified nucleosomes were identified by running a small portion of the samples on an 0.7% agarose nucleoprotein gel (40). Fractions containing mononucleosomes were dialyzed for 3 h against a buffer containing 10 mM Tris-HCl, pH 8.0.

hSWI/SNF reactions and DNase I assays. The human SWI/SNF complex was prepared as described previously (30). In a 200-μl reaction mixture, approximately 5 ng of nucleosomes was incubated with 245 ng of hSWI/SNF in 12 mM HEPES (pH 7.9)–60 mM KCl–7 mM $MgCl_2$–0.6 mM dithiothreitol–60 μM EDTA–100 ng of bovine serum albumin/μl in the presence or absence of 4 mM ATP (23). Reaction mixtures were incubated at 30°C for 15 min or for the times indicated in the figures. For DNase I assay of hSWI/SNF remodeling, nucleosomes were digested with 0.5 U of DNase I for 2 min at room temperature after incubation of nucleosomes with hSWI/SNF as described above. The naked DNA digestions were performed with 0.06 U of DNase I at room temperature for 3 min. The samples were ethanol precipitated and analyzed by sequencing gel electrophoresis and phosphorimagery.

Restriction enzyme assays. Restriction enzyme digests were performed with 10 U of *Eco*RV/μl, 10 U of *Bam*HI/μl, 0.2 U of *Bbv*I/μl, 1 U of *Rsa*I/μl, or 0.3 U of *Hha*I/μl after incubation of nucleosomes with hSWI/SNF as described above. Note that for the *Eco*RV experiments the hairpin, flap, or nicked nucleosomes were each combined with an equal amount of nucleosomes containing the native DNA fragment before the incubation with SWI/SNF as an internal reference. The samples from the *Eco*RV assay were ethanol precipitated, resuspended in formamide loading dye, and analyzed on denaturing sequencing gels. To assess the effect of histone-DNA cross-linking on *Hha*I site accessibility, nucleosomes were reconstituted with the native DNA fragment and H2BG26C-APB as described above. The nucleosomes were irradiated with 365-nm UV light (VWR LM20E transilluminator) for 25 s prior to incubation with hSWI/SNF, where indicated. Aliquots from the reaction mixtures were taken at various times, digestion was terminated with EDTA-sodium dodecyl sulfate, samples were loaded onto 6% nondenaturing polyacrylamide gels, and electrophoresis was carried out. Gels were dried and analyzed with a phosphorimager. Cross-linked DNAs were distinguished from non-cross-linked DNAs by migration on the gel (1).

Hydroxyl radical footprinting of nucleosomes. Hydroxyl radical footprinting of nucleosomes reconstituted onto native, hairpin, or flap DNA was performed by pipetting 20 μl each of 1 mM Fe-EDTA and 20 mM sodium ascorbate to the side of a tube containing 140 μl of nucleosomes. The reaction was started by pipetting 20 μl of a 0.12% solution of H_2O_2 into a drop and then quickly mixing the reagents with the nucleosomes. After 2 min, the reaction was stopped by the addition of 20 μl of 50% glycerol, and then reaction mixtures were loaded onto preparative 0.7% agarose, 1/2× Tris-borate-EDTA gels to isolate nucleosomes and naked DNA. DNA isolated from the preparative agarose gel was ethanol precipitated, resuspended in formamide loading dye, and then loaded onto a 6% denaturing polyacrylamide gel.

Exo III assays. Nucleosomes were incubated with hSWI/SNF as described above. A 1.5-μg quantity of calf thymus DNA was added to chase any SWI/SNF complex off the nucleosomes. An 0.5-U quantity of exonuclease III (Exo III) (New England Biolabs) was added to the reaction mixtures, and the reactions were stopped with EDTA-sodium dodecyl sulfate stop solution. The samples were then ethanol precipitated, resuspended in formamide loading dye, and loaded onto a 6% denaturing polyacrylamide gel.

RESULTS

Previous workers have demonstrated that the yeast SWI/SNF complex can catalyze nucleosome translocation (sliding) on a DNA fragment containing the *Xenopus* 5S nucleosome positioning element (16). Thus, we first determined if we could detect nucleosome sliding catalyzed by human SWI/SNF on a similar DNA fragment. Nucleosomes were assembled onto the 215-bp *Xenopus* 5S DNA fragment by a salt-dialysis procedure. Chemical and nuclease mapping experiments have shown that ~80% of the nucleosomes are positioned near the 5′ end of this fragment after reconstitution (4, 22, 34) (Fig. 1A). Previously, nucleosome sliding has been detected by increased protection of a restriction enzyme site located well outside of the main nucleosome position (16). We found that a *Hha*I site located about 40 bp beyond the edge of the predicted nucleosome position was accessible in the native nucleosome sample, such that about 70% of the DNA was rapidly digested with kinetics similar to that of naked DNA (Fig. 1B, Native-X, filled bar, and results not shown). Importantly, this extent of protection did not change when nucleosomes were incubated with hSWI/SNF in the absence of ATP (Fig. 1B, Native-X, open bar). However, when nucleosomes were incubated with both hSWI/SNF and ATP, protection of this site was significantly increased (Fig. 1B, Native-X, hatched bar), consistent with SWI/SNF-catalyzed sliding of a fraction of the nucleosomes to the opposite end of this DNA fragment (16). The SWI/SNF-dependent increase in protection of the *Hha*I site is contrasted by the effect of remodeling on restriction sites located within the main nucleosome position (see Fig. 4B, below). To confirm that this increase is due to nucleosome sliding, we first fixed the position of the histone octamer on the DNA by site-specific histone-DNA cross-linking (23) and then assayed the accessibility of the *Hha*I site before and after remodeling. Importantly, no significant increase in the extent of protection of the *Hha*I site was observed for nucleosomes in which a histone was covalently cross-linked to nucleosomal DNA (Fig. 1B, Native+X), strongly supporting the idea that the increase in protection is due to nucleosome sliding.

To further substantiate the idea that hSWI/SNF can induce sliding of at least a portion of the nucleosomes in the sample, we performed Exo III assays to locate the downstream edge of the nucleosome before and after remodeling (12). Exo III digests double-stranded DNA in a 3′-to-5′ direction until progress is impeded by the edge of the nucleosome core. Typically several bands separated by 10 bp are generated for each nucleosome boundary encountered (3, 12) (Fig. 3A). We find that digestion of nucleosomes reconstituted onto the native 215-bp 5S DNA fragment reveals two main translational positions, one that corresponds with the expected position, with the downstream edge of the nucleosome at approximately +75, and another with a downstream edge near base position +125 (Fig. 3A, fourth lane from left). The latter corresponds to the approximately 20 to 25% of nucleosomes that result in protection of the *Hha*I site at position +123. After remodeling by hSWI/SNF, we find that the distribution of translational positions detected by Exo III digestion is changed. The stops near +75 are diminished while a new major stop is detected just near the edge of the fragment at approximately bp +135 (Fig. 3A, fifth lane from the left). Note that this band is clearly several nucleotides shorter than the full-length undigested DNA (Fig. 3A, third lane from the left), indicating that Exo III trimming is still occurring in this sample. A second band, mapping to position +125, may be an independent nucleosome position or may be a second stop associated with the nucleosome edge at +135. Nonetheless, the pattern clearly indicates an accumulation of nucleosomes near the downstream edge of the fragment upon remodeling by hSWI/SNF.

To test if SWI/SNF-catalyzed nucleosome sliding occurs via a twist-diffusion mechanism, we assembled nucleosomes onto either of two DNA templates containing branched DNA structures (Fig. 1A). A 13-bp double-stranded flap or a 12-bp hairpin was placed near the center of the nucleosome positioning sequence within the 5S DNA fragment. The location of the junction was carefully chosen so that the branch would extend

out away from the histone surface after reconstitution. If hSWI/SNF-catalyzed nucleosome sliding occurs by a simple twist-diffusion mechanism, then the presence of the DNA branch is expected to result in severe steric clash during rotation of the DNA past the histone surface (see below). We also investigated a nicked template as an additional control for the branched DNA templates. Nucleoprotein gel analysis of nucleosomes reconstituted with the branched DNA fragments showed that the presence of the branches did not significantly alter the efficiency of reconstitution (Fig. 2A). In addition nucleosomes reconstituted with the branched and nicked DNAs had translational and rotational positioning indistinguishable from those of nucleosomes reconstituted with the native DNA fragment as determined by hydroxyl radical footprinting (Fig. 2B and results not shown). Interestingly, a small area of additional protection from hydroxyl radical cleavage was observed in the vicinity of the flap or hairpin structures within the footprint of branched DNA-containing nucleosomes (Fig. 2B, lanes 7 and 10). Finally, to investigate the overall translational distribution of nucleosomes on the branched and nicked templates, we performed quantitative restriction enzyme digestion assays (Fig. 2C). The extent of protection of sites throughout the fragment is indicative of the distribution of nucleosomes. We find that the largest protection corresponds to the previously identified major translational position on the native fragment, while much greater cleavage occurs at sites outside this main position. Moreover, the pattern of protection can be explained by three main translational positions, two of which constitute 80% of the nucleosomes at or near the expected position near the 5′ end of the fragments (5), while the third accounts for the protection observed at the *Hha*I site (Fig. 1B). Importantly, approximately the same pattern of protection from cleavage at each site is observed for the flap, hairpin, and nick nucleosomes. Thus, we conclude that the presence of the branched DNA structures does not significantly alter either the efficiency of reconstitution or the resulting translational distribution of nucleosomes.

We next determined if the presence of the branched or nicked DNAs within these nucleosomes inhibited hSWI/SNF-catalyzed nucleosome sliding by repeating the *Hha*I digestion assay on nucleosome substrates containing these DNAs. As mentioned above, about 30% of the DNA fragments in the native, unremodeled nucleosomes are resistant to *Hha*I digestion, and this fraction increases to ~40% upon hSWI/SNF-catalyzed sliding of the nucleosomes (Fig. 1B, Native-X). Importantly, we found nearly identical proportional increases in protection of the *Hha*I site upon incubation of nucleosomes containing either of the branched DNA structures with hSWI/SNF and ATP (Fig. 1B, Flap and Hairpin). Thus, hSWI/SNF-catalyzed nucleosome sliding occurs to approximately the same extent with nucleosomes containing either of the branched DNAs, the nicked DNA, or the native DNA fragment.

We also determined if hSWI/SNF-catalyzed nucleosome sliding could be detected on the branched DNA templates by Exo III digestion. Interestingly, digestion of nucleosomes reconstituted onto the flap, hairpin, or nicked templates yields strong stops centered approximately at +75 and +125, similar to those observed with the native template. In addition, a slightly greater amount of nucleosomes positioned at the very end of the fragment is also detected as a stop near +135 in these templates (Fig. 3B, C, and D, fourth lanes from left). Importantly, after remodeling by hSWI/SNF bands corresponding to the edge of the nucleosome at +75 are greatly diminished for all three templates while bands corresponding to a nucleosome edge at +135 become predominant. These results suggest that a significant fraction of nucleosomes are relocated to positions near the downstream end of the 5S fragment. While the extent of accumulation of nucleosomes on the end of the fragment appears greater in the Exo III experiments than in the *Hha*I digestion experiments, we note that the latter measures the competing effects of nucleosome remodeling and repositioning.

To determine if the presence of the branch had any effect on general remodeling of the nucleosome by the hSWI/SNF complex, we assessed remodeling by standard DNase I digestion analysis (14). When nucleosomes were incubated in the absence of remodeling activity (+hSWI/SNF −ATP) we observed the canonical 10- to 11-bp ladder of DNase I digestion products for nucleosomes assembled with the native, branch-containing, and nick DNA fragments (Fig. 4A, lanes 4). Incubation in the presence of SWI/SNF and ATP resulted in clear disruption of histone-DNA interactions in the native control nucleosome and in nucleosomes assembled with branched DNAs (Fig. 4A, lanes 5). However, we observed a small but consistent decrease in the extent of disruption of the DNase I nucleosomal cleavage pattern for both of the nucleosomes containing branched DNAs (Fig. 4A, lanes 5).

To more quantitatively analyze the extent of remodeling in the native and branched DNA-containing nucleosomes, we performed restriction enzyme accessibility assays (24, 27). Digestion of unremodeled nucleosomes with *Eco*RV shows that a majority (90 to 95%) of nucleosomes were uncut after 15 min of digestion (Fig. 4B, filled symbols), in accordance with the relatively low probability of nucleosomal DNA site exposure (29). After incubation in the presence of hSWI/SNF remodeling activity for 15 min, a substantial fraction (>60%) of the control nucleosomes containing native 5S DNA were accessible to restriction enzyme digestion (Fig. 4B, open diamonds). Likewise, SWI/SNF remodeling resulted in a significant increase in accessibility of the *Eco*RV site in nucleosomes containing the DNA flap or the hairpin (Fig. 4B, open triangles and squares, respectively). We found, however, that the extent of cleavage of nucleosomes containing the branched DNAs was consistently about 20 to 30% less than that of the native control nucleosomes.

To assess whether the differences observed between the control nucleosomes and the branched DNA nucleosomes in the *Eco*RV restriction enzyme assay were due to the branched DNA structures themselves or to the presence of a discontinuous DNA backbone remaining from the annealing process, we analyzed nucleosomes containing only a DNA nick in place of the branched structures. Interestingly, we found that the presence of a nick led to an equivalent reduction in remodeling efficiency as measured by *Eco*RV accessibility after remodeling (Fig. 4B, open circles). It is important to note that the flap, hairpin, and nick-containing nucleosomes were incubated in the same reaction tubes with native control nucleosomes in this experiment to ensure that all the substrates were exposed to identical hSWI/SNF and *Eco*RV activities (see Materials and Methods).

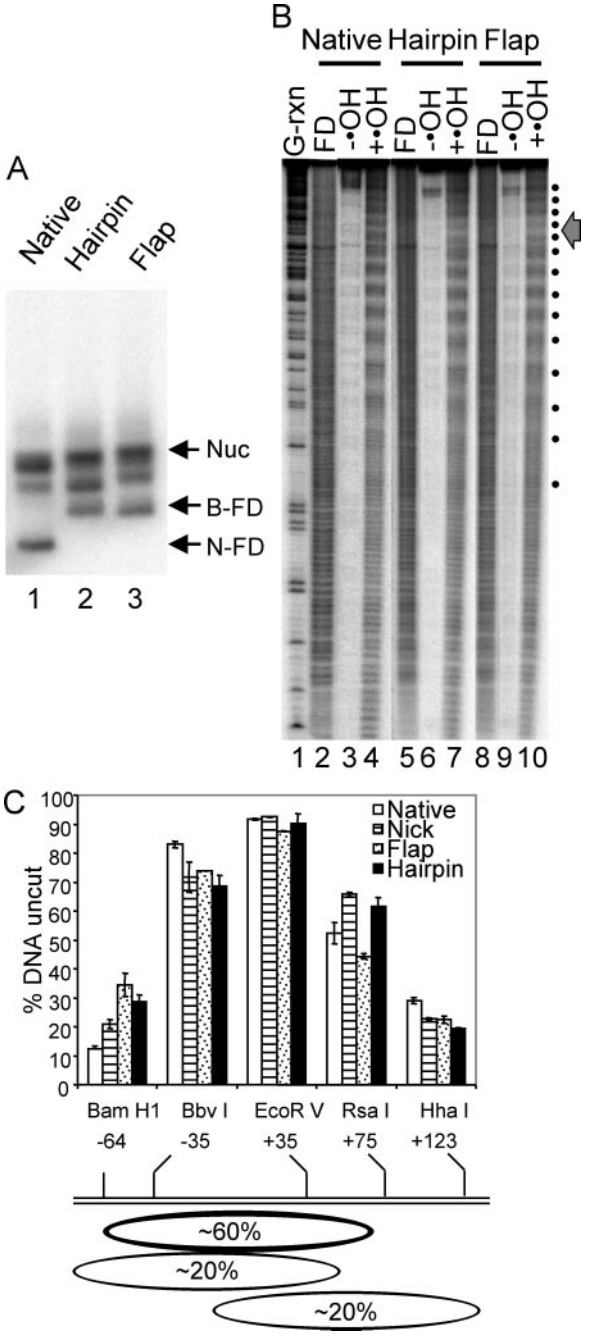

FIG. 2. Branched and nick DNAs reconstitute into canonical nucleosomes with conserved translational and rotational positioning. (A) Nucleosomes were reconstituted with either native or branched substrates and were analyzed by nucleoprotein gel electrophoresis (0.7% agarose, 1/2× Tris-borate-EDTA). Lanes 1 to 3 show nucleosome reconstitutions containing native, hairpin, and flap DNA, respectively. The positions of the native free DNA (N-FD), the branched free DNA (B-FD), and the nucleosome (Nuc) are indicated. (B) Hydroxyl radical footprinting analysis of nucleosomes containing native and branched DNA. Lane 1 shows the G-specific reaction of the 5S DNA. Lanes 2, 5, and 8 show the hydroxyl radical cleavage pattern of naked native, hairpin, and flap DNA prior to reconstitution, respectively. Lanes 3, 6, and 9 are native, hairpin, and flap DNA fragments prior to hydroxyl radical cleavage, respectively. Lanes 4, 7, and 10 show hydroxyl radical footprints of nucleosomes containing native, hairpin, and flap DNA, respectively. The 10-bp ladder cleavage pattern is indicated by the dots. The position of the branch on flap and hairpin substrates is indicated (arrow). (C) Translational positioning of native 5S DNA fragment is conserved in branched and nicked DNAs. Equal amounts of glycerol-gradient-purified nucleosomes reconstituted with either native, nicked, or branched templates were subjected to cleavage by *Bam*HI, *Bbv*I, *Eco*RV, *Rsa*I, and *Hha*I for 10 min as described in Materials and Methods. The bar graph shows the percent DNA remaining uncut after the restriction enzyme digestion in each nucleosome for each site. A distribution of translational positions that accounts for the observed protections is shown below.

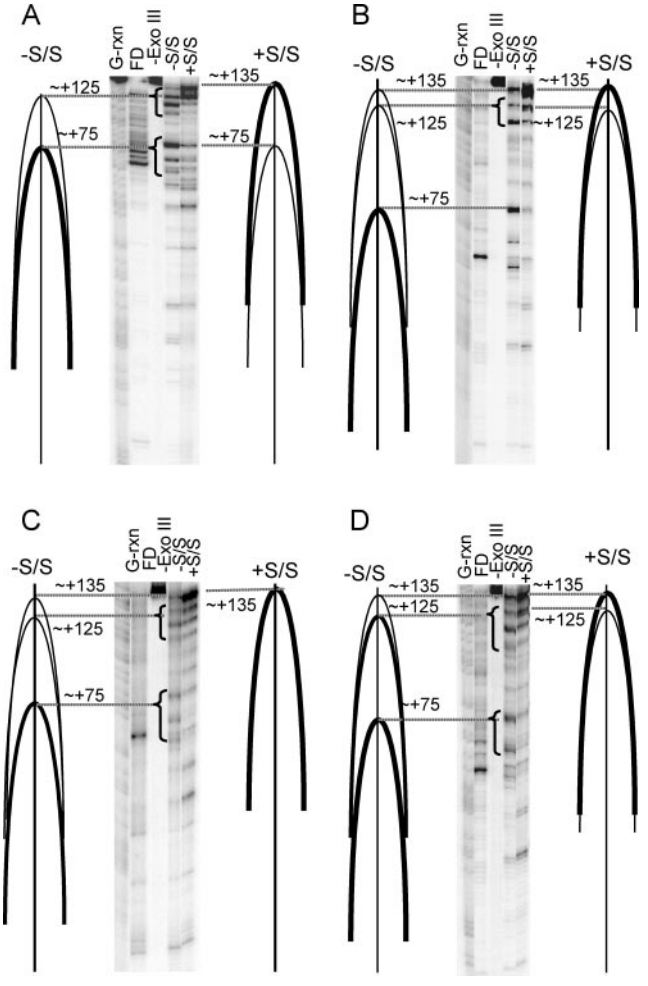

FIG. 3. Exo III analysis of nucleosome positioning before and after remodeling by hSWI/SNF. Glycerol-gradient-purified nucleosomes reconstituted with native (A), flap (B), hairpin (C), or nick (D) templates were incubated in the absence or presence of hSWI/SNF+ATP and then subjected to Exo III digestion for 5 min. Each panel shows, from left to right, G-specific cleavage of native 5S DNA as a marker, Exo III digestion pattern of naked template DNA, undigested nucleosomes, and Exo III digestion of nucleosomes before and after hSWI/SNF remodeling. The positions of the downstream edge of the nucleosomes before and after SWI/SNF remodeling are schematically represented on the left and right sides of the gel, respectively. The dark half ovals and the light ovals represent the major and minor nucleosome positions as determined from the Exo III data.

DISCUSSION

Translocation of the nucleosome along the DNA in *cis* is likely to be an important aspect of chromatin remodeling in vivo by exposing DNA target sites previously occluded by the

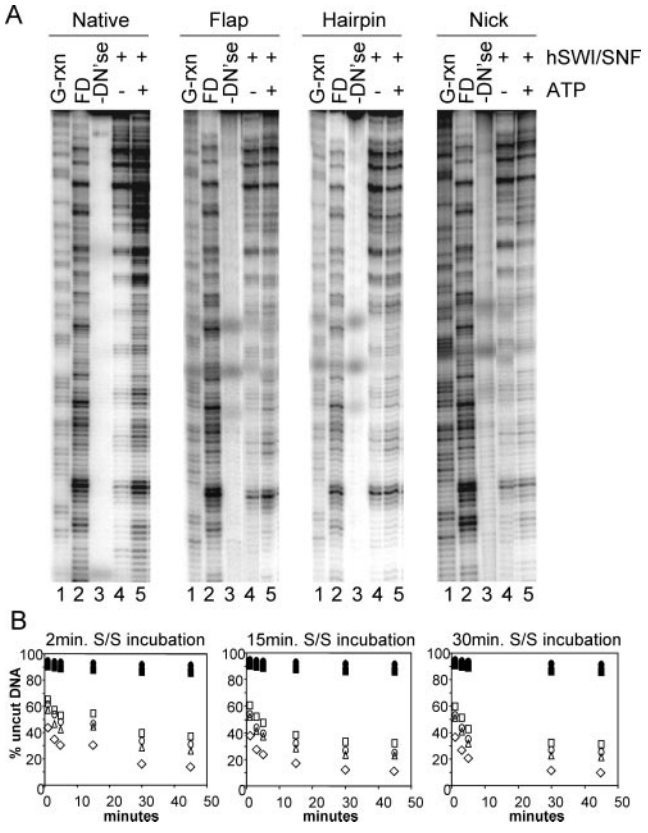

FIG. 4. hSWI/SNF remodeling of nucleosomes containing branched and nicked DNAs. (A) Analysis of hSWI/SNF remodeling of nucleosomes reconstituted with native, flap, hairpin, and nick templates by DNase I digestion. In each panel, lanes 1 show G-specific reaction markers of the native 5S DNA fragment, lanes 2 show DNase I digestion pattern of naked templates, lanes 3 are nucleosomes prior to DNase I digestion, lanes 4 show the DNase I cleavage pattern of nucleosomes incubated with hSWI/SNF without ATP, and lanes 5 show the DNase I cleavage patterns of nucleosomes incubated with hSWI/SNF and ATP for 15 min. (B) Effects of branched DNA structures on remodeling as determined by restriction enzyme accessibility assay. Glycerol-gradient-purified native, nicked, hairpin, and flap nucleosomes were incubated for the indicated times with hSWI/SNF in the presence or absence of ATP (open and solid symbols, respectively) and subjected to *Eco*RV digestion over a 45-min time course. The percent nucleosomes remaining uncut is plotted versus time of *Eco*RV digestion for native (diamonds), hairpin (squares), flap (triangles), and nicked (circles) nucleosomes.

histone octamer, allowing more efficient progression of various nuclear processes (18). Indeed, there is evidence to show that all three classes of ATP-dependent chromatin remodeling factors (SWI2/SNF2 family, ISWI family, and the Mi-2 family) are able to promote nucleosome sliding along a DNA fragment (11, 12, 16, 21, 31, 37). The mechanism(s) by which these complexes catalyze nucleosome sliding is not known but is likely to be related to the uncatalyzed (spontaneous) process.

At least two simple models have been proposed for a general sliding mechanism (reviewed in reference 37). The first involves the twisting of the DNA helix along the surface of the histone octamer much like a screw in a slot, while the second involves DNA unwrapping-recapture to form a DNA bulge, which is then transmitted around the surface of a nucleosome in a wave-like motion. We used a 215-bp 5S DNA with branched DNA structures placed near the dyad of the nucleosome to determine the mechanism of hSWI/SNF-mediated nucleosome sliding. If nucleosomes slide by incremental twisting of the DNA helix on the histone surface, the DNA flap or hairpin will sterically hinder any twisting motion of the DNA that requires the branched DNA structures to swing past the surface of the histone octamer. Thus, if hSWI/SNF-catalyzed nucleosome sliding occurs solely via a simple twist-diffusion mechanism, the presence of the DNA branched structures should drastically inhibit sliding. Moreover, if a majority of remodeling-dependent DNA site exposure requires twisting of the DNA on the nucleosome surface, then general remodeling should be severely inhibited in nucleosomes containing the branched DNA structures.

Our results indicate that hSWI/SNF-catalyzed nucleosome sliding occurs to about the same extent in the presence of the flap or hairpin as with the native DNA fragment as indicated by protection of the *Hha*I restriction enzyme site or Exo III mapping (Fig. 1B and 3). These results indicate that hSWI/SNF-catalyzed nucleosome sliding does not exclusively occur via a simple twisting-diffusion mechanism. Indeed, our results support models of sliding whereby the DNA maintains its rotational orientation with respect to the histone surface and/or partially dissociates from the nucleosome. Thus, mechanisms of sliding such as that envisioned to occur in the loop-recapture model or has been suggested to occur during polymerase invasion of the nucleosome (33) are supported by these results. However, it is important to point out that nucleosome sliding catalyzed by the action of chromatin remodeling complexes is likely to be a complicated process and may occur via a number of mechanisms (26). These processes may represent combinations of the simple twist-diffusion and loop-recapture models mentioned above or may occur via distinct mechanisms during the collapse of structurally altered, remodeled nucleosomes to canonical structures. It is also interesting that while the ySWI/SNF complex efficiently catalyzes nucleosome translocation in *cis* along DNA, this process is blocked by the presence of a stable four-way DNA junction between the original position of the nucleosome and the recipient DNA (36). This result is consistent with a model in which a loop of DNA translocates around the histone octamer and suggests that the translocating DNA must at least transiently make close, perhaps canonical, interactions with the histone octamer during sliding.

Interestingly we did observe an approximately 20 to 30% reduction in the extent of remodeling as measured by the *Eco*RV restriction enzyme accessibility assay for nucleosomes containing branched DNAs (Fig. 4B). An identical inhibition was observed in assays with nucleosomes containing only a single nick in the DNA backbone in place of the DNA branched structures. Recent results indicate that the mechanism of remodeling may involve the imposition of torsional stress upon nucleosomal DNA (10, 13). Thus, it is possible that the presence of a discontinuous DNA strand in either of the branched DNAs or the nicked DNA allows some dissipation of some torsional stress within the nucleosomal DNA during remodeling, thereby reducing the overall efficiency of the process.

It has been recently reported that the presence of a nick

within nucleosomal DNA does not inhibit ISWI-catalyzed nucleosome sliding (20). Our results are in agreement with this report and indicate that, while sliding is not affected by the presence of a nick (or a branched DNA structure), some aspects of the remodeling mechanism leading to exposure of DNA sites within the nucleosome are marginally inhibited by the presence of the nick. Still, remodeling of nicked nucleosomes is quite efficient and suggests that restriction enzyme site exposure is not dependent upon transmission of torsional stress throughout the entire nucleosomal DNA.

ACKNOWLEDGMENTS

We are grateful to G. Narlikar and R. Kingston for helpful advice and a generous gift of hSWI/SNF.

This work was supported by NIH grant RO1GM52426 and American Cancer Society grant RPG-00-080-01-GMC.

ADDENDUM IN PROOF

After submission of this work, a paper appeared by Saha et al. (A. Saha, J. Wittmeyer, and B. R. Cairns, Genes Dev. **16:**2120–2134, 2002) showing that remodeling by the yeast RSC complex as measured by restriction site accessibility assays occurs less efficiently on nucleosomes containing nicked DNA than on those containing intact DNA fragments. This result is in agreement with data presented for hSWI/SNF remodeling in Fig. 4B of our paper.

REFERENCES

1. **Aoyagi, S., G. Narlikar, C. Zheng, S. Sif, R. E. Kingston, and J. J. Hayes.** 2002. Nucleosome remodeling by the human SWI/SNF complex requires transient global disruption of histone-DNA interactions. Mol. Cell. Biol. **22:**3653–3662.
2. **Bazett-Jones, D. P., J. Côté, C. C. Landel, C. L. Peterson, and J. L. Workman.** 1999. The SWI/SNF complex creates loop domains in DNA and polynucleosome arrays and can disrupt DNA-histone contacts within these domains. Mol. Cell. Biol. **19:**1470–1478.
3. **Blomquist, P., S. Belikov, and O. Wrange.** 1999. Increased nuclear factor 1 binding to its nucleosomal site mediated by sequence-dependent DNA structure. Nucleic Acids Res. **27:**517–525.
4. **Boyer, L. A., X. Shao, R. H. Ebright, and C. L. Peterson.** 2000. Roles of the histone H2A-H2B dimers and the (H3-H4)(2) tetramer in nucleosome remodeling by the SWI-SNF complex. J. Biol. Chem. **275:**11545–11552.
5. **Chafin, D. R., J. M. Vitolo, L. A. Henricksen, R. A. Bambara, and J. J. Hayes.** 2000. Human DNA ligase I efficiently seals nicks in nucleosomes. EMBO J. **19:**5492–5501.
6. **Côté, J., C. L. Peterson, and J. L. Workman.** 1998. Perturbation of nucleosome core structure by the SWI/SNF complex persists after its detachment, enhancing subsequent transcription factor binding. Proc. Natl. Acad. Sci. USA **95:**4947–4952.
7. **Côté, J., J. Quinn, J. L. Workman, and C. L. Peterson.** 1994. Stimulation of GAL4 derivative binding to nucleosomal DNA by the yeast SWI/SNF complex. Science **265:**53–60.
8. **de la Serna, I. L., K. A. Carlson, and A. N. Imbalzano.** 2001. Mammalian SWI/SNF complexes promote MyoD-mediated muscle differentiation. Nat. Genet. **27:**187–190.
9. **Deuring, R., L. Fanti, J. A. Armstrong, M. Sarte, O. Papoulas, M. Prestel, G. Daubresse, M. Verardo, S. L. Moseley, M. Berloco, T. Tsukiyama, C. Wu, S. Pimpinelli, and J. W. Tamkun.** 2000. The ISWI chromatin-remodeling protein is required for gene expression and the maintenance of higher order chromatin structure in vivo. Mol. Cell **5:**355–365.
10. **Gavin, I., P. J. Horn, and C. L. Peterson.** 2001. SWI/SNF chromatin remodeling requires changes in DNA topology. Mol. Cell **7:**97–104.
11. **Guschin, D., P. A. Wade, N. Kikyo, and A. P. Wolffe.** 2000. ATP-dependent histone octamer mobilization and histone deacetylation mediated by the Mi-2 chromatin remodeling complex. Biochemistry **39:**5238–5245.
12. **Hamiche, A., R. Sandaltzopoulos, D. A. Gdula, and C. Wu.** 1999. ATP-dependent histone octamer sliding mediated by the chromatin remodeling complex NURF. Cell **97:**833–842.
13. **Havas, K., A. Flaus, M. Phelan, R. Kingston, P. A. Wade, D. M. Lilley, and T. Owen-Hughes.** 2000. Generation of superhelical torsion by ATP-dependent chromatin remodeling activities. Cell **103:**1133–1142.
14. **Imbalzano, A. N., H. Kwon, M. R. Green, and R. E. Kingston.** 1994. Facilitated binding of TATA-binding protein to nucleosomal DNA. Nature **370:**481–485.
15. **Imbalzano, A. N., G. R. Schnitzler, and R. E. Kingston.** 1996. Nucleosome disruption by human SWI/SNF is maintained in the absence of continued ATP hydrolysis. J. Biol. Chem. **271:**20726–20733.
16. **Jaskelioff, M., I. M. Gavin, C. L. Peterson, and C. Logie.** 2000. SWI-SNF-mediated nucleosome remodeling: role of histone octamer mobility in the persistence of the remodeled state. Mol. Cell. Biol. **20:**3058–3068.
17. **Jenuwein, T., and C. D. Allis.** 2001. Translating the histone code. Science **293:**1074–1080.
18. **Kingston, R. E., and G. J. Narlikar.** 1999. ATP-dependent remodeling and acetylation as regulators of chromatin fluidity. Genes Dev. **13:**2339–2352.
19. **Kwon, H., A. N. Imbalzano, P. A. Khavari, R. E. Kingston, and M. R. Green.** 1994. Nucleosome disruption and enhancement of activator binding by a human SW1/SNF complex. Nature **370:**477–481.
20. **Längst, G., and P. B. Becker.** 2001. Nucleosome mobilization and positioning by ISWI-containing chromatin-remodeling factors. J. Cell Sci. **114:**2561–2568.
21. **Längst, G., E. J. Bonte, D. F. Corona, and P. B. Becker.** 1999. Nucleosome movement by CHRAC and ISWI without disruption or trans-displacement of the histone octamer. Cell **97:**843–852.
22. **Lee, K. M., and J. J. Hayes.** 1997. The N-terminal tail of histone H2A binds to two distinct sites within the nucleosome core. Proc. Natl. Acad. Sci. USA **94:**8959–8964.
23. **Lee, K. M., S. Sif, R. E. Kingston, and J. J. Hayes.** 1999. hSWI/SNF disrupts interactions between the H2A N-terminal tail and nucleosomal DNA. Biochemistry **38:**8423–8429.
24. **Logie, C., and C. L. Peterson.** 1997. Catalytic activity of the yeast SWI/SNF complex on reconstituted nucleosome arrays. EMBO J. **16:**6772–6782.
25. **Luger, K., A. W. Mader, R. K. Richmond, D. F. Sargent, and T. J. Richmond.** 1997. Crystal structure of the nucleosome core particle at 2.8 A resolution. Nature **389:**251–260.
26. **Narlikar, G. J., H. Y. Fan, and R. E. Kingston.** 2002. Cooperation between complexes that regulate chromatin structure and transcription. Cell **108:**475–487.
27. **Narlikar, G. J., M. L. Phelan, and R. E. Kingston.** 2001. Generation and interconversion of multiple distinct nucleosomal states as a mechanism for catalyzing chromatin fluidity. Mol. Cell **8:**1219–1230.
28. **Peterson, C. L., and J. L. Workman.** 2000. Promoter targeting and chromatin remodeling by the SWI/SNF complex. Curr. Opin. Genet. Dev. **10:**187–192.
29. **Polach, K. J., and J. Widom.** 1995. Mechanism of protein access to specific DNA sequences in chromatin: a dynamic equilibrium model for gene regulation. J. Mol. Biol. **254:**130–149.
30. **Schnitzler, G., S. Sif, and R. E. Kingston.** 1998. Human SWI/SNF interconverts a nucleosome between its base state and a stable remodeled state. Cell **94:**17–27.
31. **Schnitzler, G. R., C. L. Cheung, J. H. Hafner, A. J. Saurin, R. E. Kingston, and C. M. Lieber.** 2001. Direct imaging of human SWI/SNF-remodeled mono- and polynucleosomes by atomic force microscopy employing carbon nanotube tips. Mol. Cell. Biol. **21:**8504–8511.
32. **Strahl, B. D., and C. D. Allis.** 2000. The language of covalent histone modifications. Nature **403:**41–45.
33. **Studitsky, V. M., D. J. Clark, and G. Felsenfeld.** 1995. Overcoming a nucleosomal barrier to transcription. Cell **83:**19–27.
34. **Thiriet, C., and J. J. Hayes.** 1998. Functionally relevant histone-DNA interactions extend beyond the classically defined nucleosome core region. J. Biol. Chem. **273:**21352–21358.
35. **Vignali, M., A. H. Hassan, K. E. Neely, and J. L. Workman.** 2000. ATP-dependent chromatin-remodeling complexes. Mol. Cell. Biol. **20:**1899–1910.
36. **Whitehouse, I., A. Flaus, B. R. Cairns, M. F. White, J. L. Workman, and T. Owen-Hughes.** 1999. Nucleosome mobilization catalysed by the yeast SWI/SNF complex. Nature **400:**784–787.
37. **Whitehouse, I., A. Flaus, K. Havas, and T. Owen-Hughes.** 2000. Mechanisms for ATP-dependent chromatin remodelling. Biochem. Soc. Trans. **28:**376–379.
38. **Wolffe, A. P.** 1998. Chromatin structure and function, 3rd ed. Academic Press, London, United Kingdom.
39. **Wolffe, A. P., and J. J. Hayes.** 1999. Chromatin disruption and modification. Nucleic Acids Res. **27:**711–720.
40. **Wolffe, A. P., and J. J. Hayes.** 1993. Transcription factor interactions with model nucleosomal templates. Methods Mol. Genet. **2:**314–330.
41. **Workman, J. L., and R. E. Kingston.** 1998. Alteration of nucleosome structure as a mechanism of transcriptional regulation. Annu. Rev. Biochem. **67:**545–579.
42. **Zhang, Y., and D. Reinberg.** 2001. Transcription regulation by histone modification: interplay between different covalent modifications of the histone tail domains. Genes Dev. **15:**2343–2360.